A High-resolution Method for Realistic Detonation Structure Simulation

R. Deiterding

Abstract. Detonation simulation is one of the computationally most challenging hyperbolic problems of practical interest. The source terms from detailed non-equilibrium chemistry are usually stiff and introduce non-neglectable scales typically not present in purely hydrodynamic calculations. This paper outlines all components of an efficient solution strategy. Emphasis is put on the description of the employed shock-capturing scheme and the necessary extensions of the underlying approximative Riemann solver for thermally perfect multi-component Euler equations. Computational results confirm effectiveness and relevancy of the approach.

1. Introduction

Detonations are shock-induced combustion waves that internally consist of a discontinuous hydrodynamic shock followed by a smooth region of decaying combustion. In a self-sustaining detonation, shock and reaction zone propagate essentially with Chapman-Jouguet (CJ) velocity, the speed of propagation for perfect energetic equilibrium. The balance between shock and reaction is fragile and smallest disturbances are sufficient to trigger symmetry breaking. Non-neglectable highly instationary triple point situations arise that need to be considered in technical applications and safety analysis. Their accurate numerical representation requires computational meshes with extraordinarily high local resolution, but in particular a robust and reliable high-resolution upwind scheme for the practically relevant thermally perfect multi-component Euler equations coupled to an implicit ordinary differential equations solver to incorporate the reaction terms. After a rough mathematical outline of the governing equations, we will focus especially on the algorithmic description of an approximative Riemann solver of Roe-type as basis of our high-resolution finite volume (FV) upwind scheme [6]. In particular, we discuss essential modifications to ensure the positivity of all quantities and to prevent unphysical instabilities along the detonation front [5, 10, 14]. Finally, highly resolved direct simulations of hydrogen-oxygen CJ detonations are presented showing extinction and reignition of combustion, and the propagation of triple points in good structural agreement with experimental results.

2. Governing Equations

The governing equations for detonation propagation in premixed gases are the Euler equations for multiple thermally perfect species with reactive source terms [17]. In d-dimensional Cartesian coordinates these equations can be written as

$$\frac{\partial}{\partial_t}\mathbf{q}(\mathbf{x},t)+\sum_{n=1}^{d}\frac{\partial}{\partial x_n}\mathbf{f}_n(\mathbf{q}(\mathbf{x},t))=\mathbf{s}(\mathbf{q}(\mathbf{x},t))\,,\quad \mathbf{x}=(x_1,...,x_d)^T\in\mathbb{R}^d\,,\quad t\in\mathbb{R}_0^+ \tag{1}$$

with $\mathbf{q}=\mathbf{q}(\mathbf{x},t)\in S\subset\mathbb{R}^M$ denoting the vector of conserved quantities, $\mathbf{f}_n(\mathbf{q})\in \mathrm{C}^1(S,\mathbb{R}^M)$, $n=1,...,d$ the flux functions, and $\mathbf{s}(\mathbf{q})\in\mathrm{C}^1(S,\mathbb{R}^M)$ the reaction term. For K species the vector of conserved quantities has $M=K+d+1$ components. We choose the form $\mathbf{q}(\mathbf{x},t)=(\rho_1,...,\rho_K,\rho u_1,...,\rho u_d,\rho E)^T$ with ρ_i denoting the partial densities and $\rho=\sum_{i=1}^K\rho_i$ the total density. The ratios $Y_i=\rho_i/\rho$ are called mass fractions. We denote the nth component of the velocity vector $\mathbf{u}=(u_1,\ldots,u_d)^T$ by u_n and E is the total energy per unit mass. The flux functions read

$$\mathbf{f}_n(\mathbf{q})=(\rho_1u_n,...,\rho_Ku_n,\rho u_1u_n+\delta_{1n}p,...,\rho u_du_n+\delta_{dn}p,u_n(\rho E+p))^T,n=1,...,d.$$

Herein, p is the hydrostatic pressure and δ_{jn} the Kronecker-Symbol. It is typically assumed that all species are ideal gases in thermal equilibrium and the same temperature T can be used to evaluate the partial pressure of all species as $p_i=\mathcal{R}T\rho_i/W_i$ with $\mathcal{R}$ denoting the universal constant and W_i the molecular weight, respectively. Each species is assumed to be *thermally perfect* and has a temperature-dependent specific heat $c_{pi}(T)$. The enthalpies per unit mass are written as $h_i(T)=h_i^0+\int_{T^0}^T c_{pi}(\sigma)d\sigma$ with h_i^0 called heat of formation at reference temperature T^0.[1] Inserting $h=\sum_{i=1}^K Y_i\,h_i(T)$ and Dalton's law for the total pressure, i.e. $p=\sum_{i=1}^K p_i$, into the thermodynamic relation $\rho h-\rho E+\rho\,\mathbf{u}^2/2-p=0$ yields

$$\varphi(\mathbf{q},T):=\sum_{i=1}^K\rho_i\,h_i(T)-\rho E+\rho\,\frac{\mathbf{u}^2}{2}-\mathcal{R}T\sum_{i=1}^K\frac{\rho_i}{W_i}=0\,. \tag{2}$$

It can be proven rigorously [2], that for each $\mathbf{q}$ in the space of admissible states S a unique temperature T exists that satisfies Eq. (2). Unfortunately, a closed form of the inverse can only be derived under simplifying assumptions and the iterative computation of T from Eq. (2) is in general unavoidable, whenever the pressure p has to be evaluated. But as $\varphi(\cdot,T)$ can be shown to be a strict monotone function in T the implementation of a reliable and efficient root finding routine is straightforward, cf. [2]. The appropriate speed of sound for the described model is the *frozen* speed of sound, which is given by $c^2=\sum_{i=1}^K Y_i\,\phi_i-(\gamma-1)\left(\mathbf{u}^2-H\right)$ with $H=h+\mathbf{u}^2/2$ and $\phi_i:=(\gamma-1)\left(\mathbf{u}^2/2-h_i(T)\right)+\gamma\mathcal{R}T/W_i$, where γ can be calculated

[1] In order to speed up the evaluation of $c_{pi}(T)$ and $h_i(T)$, which are typically given by polynomial approximations of fourth order [9], look-up tables are constructed during startup of the computational code. They store $c_{pi}(T)$ and $h_i(T)$ for all integers in the valid temperature range and intermediate values are interpolated.

from the mixture quantities $c_p = \sum_{i=1}^{K} Y_i\, c_{pi}(T)$ and $W = (\sum_{i=1}^{K} Y_i/W_i)^{-1}$ by $\gamma = c_p(c_p - \mathcal{R}/W)^{-1}$.

The Euler equations for thermally perfect gas-mixtures inherit most mathematical properties of the standard Euler equations for a single polytropic gas with equation of state $p = (\gamma-1)\left(\rho E - \rho\,\mathbf{u}^2/2\right)$. The proof of hyperbolicity is straightforward [2], and for instance in two space dimensions the matrix of right eigenvectors $\mathbf{R}_1(\mathbf{q}) = (\mathbf{r}_1|\ldots|\mathbf{r}_{K+d+1})$ that diagonalizes $\mathbf{A}_1(\mathbf{q})$ with $\mathbf{R}_1^{-1}(\mathbf{q})\,\mathbf{A}_1(\mathbf{q})\,\mathbf{R}_1(\mathbf{q}) = \mathbf{\Lambda}_1(\mathbf{q})$ for all $\mathbf{q} \in S$ with $\mathbf{\Lambda}_1(\mathbf{q}) = \mathrm{diag}(u_1 - c, u_1, \ldots, u_1, u_1 + c)$ takes the form

$$\mathbf{R}_1(\mathbf{q}) = \begin{bmatrix} Y_1 & 1 & 0 & \ldots & & 0 & 0 & Y_1 \\ & 0 & & & & : & & \\ \vdots & : & & \ddots & & 0 & \vdots & \vdots \\ Y_K & 0 & & \ldots & 0 & 1 & 0 & Y_K \\ u_1 - c & u_1 & & \ldots & & u_1 & 0 & u_1 + c \\ u_2 & u_2 & & \ldots & & u_2 & 1 & u_2 \\ H - u_1 c & \mathbf{u}^2 - \dfrac{\phi_1}{\gamma-1} & & \ldots & & \mathbf{u}^2 - \dfrac{\phi_K}{\gamma-1} & u_2 & H + u_1 c \end{bmatrix}. \tag{3}$$

For $\mathbf{s} \equiv \mathbf{0}$ the solution structure of a quasi-one-dimensional Riemann Problem can be shown to be in principle identical to the standard case of a single polytropic gas. The first and last characteristic field with the eigenvalues $u_n - c$ and $u_n + c$ are genuinely nonlinear, provided that the condition $\frac{\gamma(\gamma+1)}{(1-\gamma)T} \neq \frac{\partial\gamma}{\partial T}$ is satisfied for all $\mathbf{q} \in S$ [2]. All other characteristic fields are associated to the eigenvalue u_n and are linearly degenerate.

Realistic combustion is modeled with a source term of the form $\mathbf{s}(\mathbf{q}) = (W_1\,\dot\omega_1, ..., W_K\,\dot\omega_K, 0, ..., 0, 0)^T$, where the chemical production rate for each species is derived from a reaction mechanism of J chemical reactions as

$$\dot\omega_i = \sum_{j=1}^{J} (\nu_{ji}^r - \nu_{ji}^f)\left[k_j^f \prod_{l=1}^{K}\left(\frac{\rho_l}{W_l}\right)^{\nu_{jl}^f} - k_j^r \prod_{l=1}^{K}\left(\frac{\rho_l}{W_l}\right)^{\nu_{jl}^r}\right],\ i = 1, ..., K\ . \tag{4}$$

In the latter, $\nu_{ji}^{f/r}$ denote the forward and backward stoichiometric coefficients of the ith species in the jth reaction. The rate expressions are evaluated by the Arrhenius law $k_j^{f/r}(T) = A_j^{f/r} T^{\beta_j^{f/r}} \exp(-E_j^{f/r}/\mathcal{R}T)$, cf. [17].[2]

3. Numerical Methods

Detailed chemical reaction mechanisms suitable for ignition and extinction phenomena typically involve temporal scales significantly smaller than those present in the resulting hydrodynamic transport. In order to derive an efficient numerical method for (1) we therefore employ a time-operator splitting approach and decouple convection and chemical reaction numerically [12]. The homogeneous partial

[2]We enhance the evaluation of (4) in our computational code by employing highly efficient mechanism-specific routines that are produced by a straightforward automatic source code generator on top of the Chemkin-II library [9] in advance, see [2] for details.

differential equation

$$\frac{\partial \mathbf{q}}{\partial t} + \sum_{n=1}^{d} \frac{\partial}{\partial x_n} \mathbf{f}_n(\mathbf{q}) = 0 \tag{5}$$

and the usually stiff system of ordinary differential equations

$$\mathcal{S}^{(\Delta t)}: \quad \partial_t \rho_i = W_i \dot{\omega}_i \left(\rho_1, \ldots, \rho_K, T\right) \ , \quad i = 1, \ldots, K \tag{6}$$

are integrated successively with the data from the preceding step as initial condition. We use a robust implementation of a semi-implicit Rosenbrock-Wanner method of fourth order with automatic temporal stepsize adjustment [8] to solve (6) with initial condition $\rho_i(0) = \rho Y_i^0$, $i = 1, ..., K$ in every FV cell. Total density ρ, specific energy E and velocities u_n remain unchanged, which corresponds to a reaction in an adiabatic constant volume environment. In order to construct a robust and reliable FV scheme for Eq. (5) we apply the idea of operator splitting also to Eq. (5). For simplicity, we assume an equidistant discretization in two space dimensions with mesh widths Δx_1, Δx_2 and a constant time step Δt:

$$\mathcal{X}_1^{(\Delta t)}: \ \tilde{\mathbf{Q}}_{jk}^{\kappa+\frac{1}{2}} = \mathbf{Q}_{jk}^{\kappa} - \frac{\Delta t}{\Delta x_1} \left[\mathbf{F}^1(\mathbf{Q}_{j-\nu+1,k}^{\kappa}, ..., \mathbf{Q}_{j+\nu,k}^{\kappa}) - \mathbf{F}^1(\mathbf{Q}_{j-\nu,k}^{\kappa}, ..., \mathbf{Q}_{j+\nu-1,k}^{\kappa}) \right] ,$$

$$\mathcal{X}_2^{(\Delta t)}: \ \tilde{\mathbf{Q}}_{jk}^{\kappa+1} = \tilde{\mathbf{Q}}_{jk}^{\kappa+\frac{1}{2}} - \frac{\Delta t}{\Delta x_2} \left[\mathbf{F}^2(\tilde{\mathbf{Q}}_{j,k-\nu+1}^{\kappa+\frac{1}{2}}, ..., \tilde{\mathbf{Q}}_{j,k+\nu}^{\kappa+\frac{1}{2}}) - \mathbf{F}^2(\tilde{\mathbf{Q}}_{j,k-\nu}^{\kappa+\frac{1}{2}}, ..., \tilde{\mathbf{Q}}_{j,k+\nu-1}^{\kappa+\frac{1}{2}}) \right]$$

The entire splitting method reads $\mathbf{Q}^{\kappa+1} = \mathcal{S}^{(\Delta t)} \mathcal{X}_2^{(\Delta t)} \mathcal{X}_1^{(\Delta t)} (\mathbf{Q}^{\kappa})$. The latter scheme is formally only first-order accurate, but it usually gives very satisfactory results, if high-resolution shock-capturing schemes are employed for the operators $\mathcal{X}_n^{(\Delta t)}$. For the upwind method of Algorithm 1, the described splitting is stable under the condition $\max_{j,k} \left(S_{j+\frac{1}{2},k} \frac{\Delta t}{\Delta x_1} \, , \, S_{j,k+\frac{1}{2}} \frac{\Delta t}{\Delta x_2} \right) \leq 1$ with $S_{j+\frac{1}{2},k}$, $S_{j,k+\frac{1}{2}}$ denoting the maximal signal speeds in both space directions according to step (S12).

3.1. Upwind Scheme

The application of dimensional splitting for the discretization of Eq. (5) has in particular the advantage that only a single quasi-one-dimensional operator $\mathcal{X}_n^{(\Delta t)}$ needs to be considered to construct a robust and reliable method. It has to be underlined that essential properties, like the ensured positivity of all quantities will typically not be preserved throughout fully multi-dimensional approaches, cf. [2].

We build our high-resolution upwind scheme around a first-order Godunov-type method that solves the Riemann Problem (RP) between two neighboring cell values $\mathbf{Q}_l$ and $\mathbf{Q}_r$ approximately, which we formulate exemplary for the x_1-direction. The method is based on an extension of Roe's linearized Riemann solver for Euler equations for a single polytropic gas for multiple thermally perfect species by Grossman and Cinella [6] that corresponds to the steps (S1) to (S7) in Algorithm 1. The structure of the Roe-averaged right eigenvectors $\hat{\mathbf{r}}_m$ is given in Eq. (3). In (S8), (S9) the two intermediate states of the linearized RP are evaluated and the intrinsic problem of negative total densities and internal energies near vacuum

(S1) Calculate $\hat{\rho} = \sqrt{\rho_l \rho_r}$ and $\hat{v} = \frac{\sqrt{\rho_l} v_l + \sqrt{\rho_r} v_r}{\sqrt{\rho_l} + \sqrt{\rho_r}}$ for u_n, Y_i, H, h_i, T.

(S2) Compute $\hat{\gamma} = \hat{c}_p (\hat{c}_p - \mathcal{R}/\hat{W})^{-1}$ with $\hat{W} = (\sum_{i=1}^{K} \hat{Y}_i / W_i)^{-1}$ and $\hat{c}_{pi} = \dfrac{1}{T_r - T_l} \displaystyle\int_{T_l}^{T_r} c_{pi}(\sigma)\, d\sigma$.

(S3) Calculate $\hat{\phi}_i = (\hat{\gamma} - 1) \left(\hat{\mathbf{u}}^2/2 - \hat{h}_i \right) + \hat{\gamma}\, \mathcal{R}\, \hat{T}/W_i$.

(S4) Calculate $\hat{c} = \left(\sum_{i=1}^{K} \hat{Y}_i\, \hat{\phi}_i - (\hat{\gamma} - 1)(\hat{\mathbf{u}}^2 - \hat{H}) \right)^{1/2}$.

(S5) Use $\Delta \mathbf{Q} = \mathbf{Q}_r - \mathbf{Q}_l$ and Δp to compute the wave strengths

$$a_{1,K+d+1} = \frac{\Delta p \mp \hat{\rho} \hat{c} \Delta u_1}{2\hat{c}^2}\ ,\ a_{1+i} = \Delta \rho_i - \hat{Y}_i \frac{\Delta p}{\hat{c}^2}\ ,\ a_{K+n} = \hat{\rho} \Delta u_n .$$

(S6) Calculate $\mathbf{W}_1 = a_1 \hat{\mathbf{r}}_1$, $\mathbf{W}_2 = \displaystyle\sum_{m=2}^{K+d} a_m \hat{\mathbf{r}}_m$, $\mathbf{W}_3 = a_{K+d+1} \hat{\mathbf{r}}_{K+d+1}$.

(S7) Evaluate $s_1 = \hat{u}_1 - \hat{c}$, $s_2 = \hat{u}_1$, $s_3 = \hat{u}_1 + \hat{c}$.

(S8) Evaluate $\rho^\star_{l/r}$, $u^\star_{1,l/r}$, $e^\star_{l/r}$, $c^\star_{1,l/r}$ from $\mathbf{Q}^\star_l = \mathbf{Q}_l + \mathbf{W}_1$ and $\mathbf{Q}^\star_r = \mathbf{Q}_r - \mathbf{W}_3$.

(S9) If $\rho^\star_{l/r} \le 0$ or $e^\star_{l/r} \le 0$ set $s_1 = \min(u_{1,l} - c_l, u_{1,r} - c_r)$, $s_3 = \max(u_{1,l} + c_l, u_{1,r} + c_r)$, use HLL flux

$$\mathbf{F}(\mathbf{Q}_l, \mathbf{Q}_r) = \begin{cases} \mathbf{f}(\mathbf{Q}_l), & 0 < s_1\ , \\ \frac{s_3 \mathbf{f}(\mathbf{Q}_l) - s_1 \mathbf{f}(\mathbf{Q}_R) + s_1 s_3 (\mathbf{Q}_r - \mathbf{Q}_l)}{s_3 - s_1}, & s_1 \le 0 \le s_3\ , \\ \mathbf{f}(\mathbf{Q}_r), & 0 > s_3\ , \end{cases}$$

and go to (S12).

(S10) Evaluate Roe flux $\mathbf{F}(\mathbf{Q}_l, \mathbf{Q}_r) = \frac{1}{2} \left(\mathbf{f}(\mathbf{Q}_l) + \mathbf{f}(\mathbf{Q}_r) - \sum_{\iota=1}^{3} |\bar{s}_\iota| \mathbf{W}_\iota \right)$ with entropy enforcement formula

$$|\bar{s}_\iota| = \begin{cases} |s_\iota|\ , & |s_\iota| \ge 2\eta\ , \\ |s_\iota^2|/(4\eta) + \eta\ , & |s_\iota| < 2\eta\ . \end{cases} \tag{7}$$

(S11) With $\mathbf{F}_\rho := \sum_{i=1}^{K} \mathbf{F}_i$ replace $\mathbf{F}_i$ by $\bar{\mathbf{F}}_i = \mathbf{F}_\rho \cdot \begin{cases} Y_i^l\ , & \mathbf{F}_\rho \ge 0\ , \\ Y_i^r\ , & \mathbf{F}_\rho < 0\ . \end{cases}$

(S12) Evaluate maximal signal speed by $S = \max(|s_1|, |s_3|)$.

Algorithm 1. Hybrid Roe-HLL scheme for detonation simulation.

due to the Roe linearization, cf. [5], is circumvented by switching in case of an unphysical approximation in the intermediate states to the simple, but extremely robust Harten-Lax-Van Leer (HLL) Riemann solver. If Roe's flux approximation is applied in step (S10), violations of the entropy condition are generally avoided by adding an appropriate amount of numerical viscosity [7]. A natural choice for the parameter η for Euler equations is $\eta = \frac{1}{2}(|u_{1,r} - u_{1,l}| + |c_r - c_l|)$, cf. [14].

In one space-dimension, Eq. (7) only needs to be applied to $\iota = 1, 3$ and $\bar{s}_2 = s_2$ can be used, but two- and three-dimensional detonation simulations usually

require the extension of Eq. (7) to $\iota = 2$. The shock of typical detonation waves is extraordinarily strong and its approximation is often corrupted by the carbuncle phenomenon, a multi-dimensional numerical crossflow instability that occurs at strong grid-aligned shocks or detonation waves [13]. The carbuncle phenomenon can be avoided completely by applying Eq. (7) to all characteristic fields and evaluating η in a multi-dimensional way. We have successfully utilized the "H-correction" of Sanders et al. [14] for this purpose. For instance in the x_2-direction in two space dimensions it reads

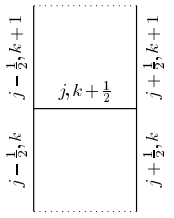

FIGURE 1. H-correction between (j,k) and $(j,k+1)$.

$$\bar{\eta}_{j,k+\frac{1}{2}} = \max\left\{\eta_{j+\frac{1}{2},k}, \eta_{j-\frac{1}{2},k}, \eta_{j,\,k+\frac{1}{2}}, \eta_{j-\frac{1}{2},\,k+1}, \eta_{j+\frac{1}{2},\,k+1}\right\},$$

compare Fig. 1. Step (S11) ensures the positivity of the mass fractions Y_i, if the Roe approximation is applied [10]. The HLL scheme can be proven to be positivity preserving in Y_i and does not require this step, cf. [2]. A detailed derivation of the entire Roe-HLL scheme and thorough numerical comparisons with various standard methods can also be found in [2].

The hybrid Riemann solver is extended to a high-resolution method with the MUSCL-Hancock variable extrapolation technique by Van Leer [16]. The technique uses a five-point stencil with $\nu = 2$. In contrast to the Euler equations for a single polytropic gas, the extrapolation for the Euler equations of Sec. 2 can not be formulated completely in conservative variables, because the solvability of the nonlinear equation (2) can not be guaranteed for an extrapolated vector of state. The same argument is true for characteristic reconstruction techniques. We recommend to apply the MUSCL extrapolation to ρ, p, Y_i and ρu_n and to derive a thermodynamically consistent extrapolated vector of state from those. Additionally, we restrict the limiter values for Y_i such that the property $\sum_{i=1}^{K} Y_i = 1$ remains preserved for the MUSCL extrapolated values. See [2] for details.

3.2. Adaptive Mesh Refinement

Although the described shock-capturing scheme has excellent high-resolution capabilities, in particular for quasi-stationary detonations under Galilean transformation [2], it necessarily has to be used on computational meshes that are able to represent the strong local flow changes due to the reaction correctly. In order to supply the required temporal and spatial resolution efficiently, we employ the blockstructured dynamic adaptive mesh refinement (AMR) method after Berger and Colella [1]. We have implemented the AMR method in an extensively validated equation- and dimension-independent object-oriented framework. It is called AMROC (Adaptive Mesh Refinement in Object-oriented C++) and is free of charge for scientific use [4]. An efficient locality-preserving rigorous domain decomposition strategy has been realized and allows computations on large distributed memory computer systems, see [3] for details.

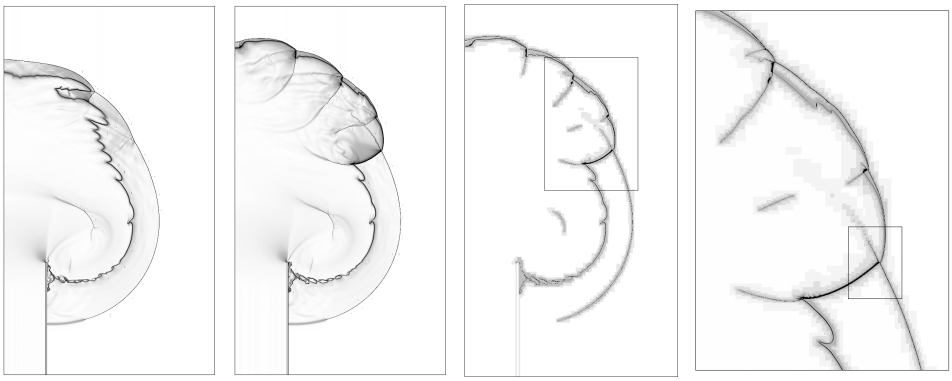

FIGURE 2. Left side: Schlieren plots of ρ. Detonation failure for tube width 8λ (left), reignition for $w = 10\lambda$ (right). Right side: Isolines of ρ on four refinement levels (shaded gray) for $w = 10\lambda$.

4. Structure of Diffracting Detonations

Experiments have shown that the behavior of planar CJ detonations propagating out of tubes into unconfinement is determined mainly by the tube width w. Some configurations exhibit triple point trajectories that form regular *detonation cells* of characteristic length and width λ. It has been found experimentally that the critical tube width for rectangular tubes is around 10λ [11], which means that for widths significantly below 10λ the process of shock wave diffraction causes a pressure decrease below the limit of detonability across the entire tube width. Hydrodynamic shock and reaction front decouple and the detonation decays to a shock-induced flame. While the successful transmission of the detonation is hardly disturbed for tubes widths $\gg 10\lambda$, a backward-facing combustion wave reignites the detonation in the partially decoupled region for widths of $\approx 10\lambda$ and creates considerable vortices.

Adaptive simulations for stoichiometric $H_2 : O_2 : Ar$ detonations on a base grid of 508×288 cells and with four additional levels with refinement factor of 2, 2, 2, and 4 in space and time perfectly reproduce experimental structure observations [15]. Initial conditions and the employed reaction mechanism of 34 elementary reactions for the 9 species H, O, OH, H_2, O_2, H_2O, HO_2, H_2O_2, and Ar are discussed in detail in [2]. The schlieren graphics of Fig. 2 clearly show the extinction of the detonation for the width $w = 8\lambda$ and the reignition wave for $w = 10\lambda$. The original confined but now diverging triple points are clearly visible for $w = 10\lambda$. These computations correspond to a uniform grid with $\approx 150\,\text{M}$ cells. At the final time $t_{end} = 240\,\mu\text{s}$ the larger run for $w = 10\lambda$ uses only $\approx 3.0\,\text{M}$ cells on all levels, which is visualized in the right side of Fig. 2. It is interesting to note that the switching to HLL according to (S9) in Algorithm 1 is only necessary in the single cell directly below the tube outlet, but occurs almost throughout the entire computation.

5. Conclusions

We have outlined a dynamically adaptive shock-capturing method applicable to realistic and practically relevant detonation structure simulation. The construction of the underlying high-resolution upwind scheme for thermally perfect gas-mixtures considers all physically necessary correction steps. The method is equally suited for detailed non-equilibrium combustion and for simplified reaction models, and is therefore useful to eliminate previously existing numerical uncertainties in computational combustion research.

References

[1] M. Berger and P. Colella. Local adaptive mesh refinement for shock hydrodynamics. *J. Comput. Phys.*, 82:64–84, 1988.

[2] R. Deiterding. *Parallel adaptive simulation of multi-dimensional detonation structures*. PhD thesis, Brandenburgische Technische Universität Cottbus, Sep 2003.

[3] R. Deiterding. Construction and application of an AMR algorithm for distributed memory computers. In T. Plewa, T. Linde, and V. G. Weirs, editors, *Proc. of Chicago Workshop on Adaptive Mesh Refinement Methods*, volume 41 of *Lecture Notes in Computational Science and Engineering*. Springer, 2005.

[4] R. Deiterding. AMROC. Available at http://amroc.sourceforge.net, Feb 2005.

[5] B. Einfeldt, C. D. Munz, P. L. Roe, and B. Sjögreen. On Godunov-type methods near low densities. *J. Comput. Phys.*, 92:273–295, 1991.

[6] B. Grossmann and P. Cinella. Flux-split algorithms for flows with non-equilibrium chemistry and vibrational relaxation. *J. Comput. Phys.*, 88:131–168, 1990.

[7] A. Harten. High resolution schemes for hyperbolic conservation laws. *J. Comput. Phys.*, 49:357–393, 1983.

[8] P. Kaps and P. Rentrop. Generalized Runge-Kutta methods of order four with stepsize control for stiff ordinary differential equations. *Num. Math.*, 33:55–68, 1979.

[9] R. J. Kee, F. M. Rupley, and J. A. Miller. *Chemkin-II: A Fortran chemical kinetics package for the analysis of gas-phase chemical kinetics*. SAND89-8009, Sandia National Laboratories, Livermore, California, Sep 1989.

[10] B. Larrouturou. How to preserve the mass fractions positivity when computing compressible multi-component flows. *J. Comput. Phys.*, 95:59–84, 1991.

[11] J. H. S. Lee. Dynamic parameters of gaseous detonations. *Ann. Rev. Fluid Mech.*, 16:311–336, 1984.

[12] E. S. Oran and J. P. Boris. *Numerical simulation of reactive flow*. Cambridge Univ. Press, Cambridge, 2nd edition, 2001.

[13] J. J. Quirk. Godunov-type schemes applied to detonation flows. In J. Buckmaster, editor, *Combustion in high-speed flows: Proc. Workshop on Combustion, Oct 12-14, 1992, Hampton*, pages 575–596, Dordrecht, 1994. Kluwer Acad. Publ.

[14] R. Sanders, E. Morano, and M.-C. Druguett. Multidimensional dissipation for upwind schemes: Stability and applications to gas dynamics. *J. Comput. Phys.*, 145:511–537, 1998.

[15] E. Schultz. *Detonation diffraction through an abrupt area expansion*. PhD thesis, California Institute of Technology, Pasadena, California, April 2000.

[16] B. van Leer. Towards the ultimate conservative difference scheme V. A second order sequel to Godunov's method. *J. Comput. Phys.*, 32:101–136, 1979.

[17] F. A. Williams. *Combustion theory*. Addison-Wesley, Reading, Massachusetts, 1985.

California Institute of Technology
1200 East California Blvd., Mail-Code 158-78, Pasadena, CA 91125, USA
E-mail address: ralf@cacr.caltech.edu